



OPEN ACCESS

EDITED BY

Paul Stevenson,
University of Surrey, United Kingdom

REVIEWED BY

Tuhin Malik,
University of Coimbra, Portugal
Serkan Akkoyun,
Cumhuriyet University, Türkiye

*CORRESPONDENCE

X. H. Wu,
✉ wuxinhui@pku.edu.cn

SPECIALTY SECTION

This article was submitted to
Nuclear Physics,
a section of the journal
Frontiers in Physics

RECEIVED 04 October 2022

ACCEPTED 14 February 2023

PUBLISHED 27 February 2023

CITATION

Wu XH (2023), Studies of different kernel
functions in nuclear mass predictions
with kernel ridge regression.
Front. Phys. 11:1061042.
doi: 10.3389/fphy.2023.1061042

COPYRIGHT

© 2023 Wu. This is an open-access article
distributed under the terms of the
[Creative Commons Attribution License](#)
(CC BY). The use, distribution or
reproduction in other forums is
permitted, provided the original author(s)
and the copyright owner(s) are credited
and that the original publication in this
journal is cited, in accordance with
accepted academic practice. No use,
distribution or reproduction is permitted
which does not comply with these terms.

Studies of different kernel functions in nuclear mass predictions with kernel ridge regression

X. H. Wu*

State Key Laboratory of Nuclear Physics and Technology, School of Physics, Peking University, Beijing, China

The kernel ridge regression (KRR) approach has been successfully applied in nuclear mass predictions. Kernel function plays an important role in the KRR approach. In this work, the performances of different kernel functions in nuclear mass predictions are carefully explored. The performances are illustrated by comparing the accuracies of describing experimentally known nuclei and the extrapolation abilities. It is found that the accuracies of describing experimentally known nuclei in the KRR approaches with most of the adopted kernels can reach the same level around 195 keV, and the performance of the Gaussian kernel is slightly better than other ones in the extrapolation validation for the whole range of the extrapolation distances.

KEYWORDS

nuclear mass, machine-learning, kernel ridge regression, kernel function, hyperparameter

1 Introduction

Nuclear mass is important for both nuclear physics [1] and astrophysics [2, 3]. During the past decades, great progress has been made in mass measurements of atomic nuclei, and about 2,500 nuclear masses have been measured to date [4]. Nevertheless, the masses of a large number of neutron-rich nuclei involved in the r -process remain unknown from experiments and cannot be measured even with the next-generation RIB facilities. Therefore, theoretical predictions for nuclear masses are imperative at the present time. Global mass model can be traced back to the von Weizsäcker mass formula based on the famous liquid drop model (LDM) [5]. Lots of efforts have been made in pursuing different possible extensions of the LDM, which are known as the macroscopic-microscopic models, such as the finite-range droplet model (FRDM) [6] and the Weizsäcker-Skyrme (WS) model [7]. The microscopic mass models based on the non-relativistic and relativistic density functional theories (DFTs) have also been developed [8–17]. The root-mean-square (rms) deviation between theoretical mass models and the available experimental data [4] range from about 3 MeV for the BW model [18] to about 300 keV for the WS ones [7], which is still not sufficient for accurate studies of exotic nuclear structure and astrophysical nucleosynthesis [19, 20]. What's more, for neutron-rich nuclei far away from the experimentally known region, the differences among the predictions of different mass models can be as large as several tens MeV [6–11, 21–23].

Machine learning (ML) has been successfully applied in various fields of physics [24, 25]. For nuclear physics, ML applications can be traced back to early 1990s [26, 27], and recently, it has been widely adopted to nuclear masses [28–41], charge radii [36, 42–45], decays and

reactions [46–53], ground and excited states [54–58], nuclear landscape [59, 60], fission yields [61–63], nuclear liquid-gas phase transition [64], variational calculations [65, 66], nuclear energy density functional [67], etc. In nuclear mass studies, ML approaches, such as the radial basis function (RBF) approach [28, 29, 68–71], the Bayesian neural network (BNN) approach [31–33, 72], and the kernel ridge regression (KRR) approach [36, 37, 41, 73], have been employed to further improve the accuracies of nuclear mass models. By training the machine learning network with the mass model residuals, i.e., deviations between experimental and calculated masses, machine learning approaches can significantly reduce the corresponding rms deviation to below 200 keV.

The KRR approach was employed to improve nuclear mass predictions for the first time in Ref. [36]. It is shown that the extrapolation behavior of the KRR approach is quite different with other approaches, e.g., the RBF approach. The RBF approach would worsen the mass descriptions for nuclei at large extrapolation distances, as the effects of the adopted linear kernel remain large at such distances. However, the KRR approach can automatically identify the limit of the extrapolation distance and avoid the risk of worsening the mass description for nuclei at large extrapolation distances, which is due to the decay behavior of the Gaussian kernel as the increase of extrapolation distance. This reflects the importance of kernel function in nuclear mass predictions with kernel-based machine learning approaches.

There are many commonly-used kernel functions in the KRR approach. The detail features of different kernels are different, which can affect the performances of the KRR approach in nuclear mass predictions. It is therefore necessary to study the effects of different kernel functions on the performances of the KRR approach in the practical applications of nuclear mass predictions.

In this work, the performances of the KRR approach for nuclear mass predictions with different kernel functions, including Gaussian, Laplacian, Matern, Cachy, Multiquadric, inverse Multiquadric, Logarithm, power, and inverse power kernels, are compared. The paper is organized as follows: In Section 2, the theoretical framework of the KRR approach is introduced. The numerical details are given in Section 3. In Section 4, the comparisons through the leave-one-out cross-validation and extrapolation validation are presented. Finally, a summary is given in Section 5.

2 Theoretical framework

The KRR approach is a powerful machine-learning approach for non-linear regression and has been successfully applied in nuclear mass predictions [36]. In this method, the KRR function is written as

$$S(\mathbf{x}_j) = \sum_{i=1}^m K(\mathbf{x}_j, \mathbf{x}_i) w_i, \quad (1)$$

where $\mathbf{x}_i \equiv (N_i, Z_i)$ are locations of nuclei in the nuclear chart, m is the number of training nuclei, w_i are weight parameters to be determined, $K(\mathbf{x}_j, \mathbf{x}_i)$ is the kernel function, which measures the correlations between nuclei. The weight parameters w_i are determined by minimizing the loss function defined as

$$L(\mathbf{w}) = \sum_{i=1}^m [S(\mathbf{x}_i) - y(\mathbf{x}_i)]^2 + \lambda \|\mathbf{w}\|^2, \quad (2)$$

where $\mathbf{w} = (w_1, \dots, w_m)$. The first term of Eq. 2 is the variance between the data $y(\mathbf{x}_i)$ and the KRR prediction $S(\mathbf{x}_i)$, and the second is the penalty term that penalizes large weights to reduce the risk of overfitting. The hyperparameter λ determines the strength of penalty. Minimizing Eq. 2 yields

$$\mathbf{w} = (\mathbf{K} + \lambda \mathbf{I})^{-1} \mathbf{y}, \quad (3)$$

where \mathbf{K} is the kernel matrix with elements $K_{ij} = K(\mathbf{x}_i, \mathbf{x}_j)$, and \mathbf{I} is the identity matrix.

Nine kernel functions are adopted in the present study, i.e., the Gaussian kernel $K(r) = \exp(-r^2/2\sigma^2)$, the Laplacian kernel $K(r) = \exp(-r/\sigma)$, the Matern kernel $K(r) = (1 + 3r/5\sigma) \exp(-3r/5\sigma)$, the Cachy kernel $K(r) = 1/(1 + r^2/\sigma)$, the Multiquadric (MQ) kernel $K(r) = \sqrt{r^2 + \sigma^2}$, the inverse MQ kernel $K(r) = 1/\sqrt{r^2 + \sigma^2}$, the Logarithm kernel $K(r) = \ln(r^\sigma + 1)$, the power kernel $K(r) = r^\sigma$, and the inverse power kernel $K(r) = 1/r^\sigma$, where the Euclidean norm $r = \|\mathbf{x}_i - \mathbf{x}_j\| = \sqrt{(N_i - N_j)^2 + (Z_i - Z_j)^2}$ is defined to be the distance between two nuclei. The adjustable hyperparameter $\sigma \geq 0$ in each kernel plays an important role in the performance of the corresponding kernel, and should be carefully tuned according to the nuclear mass data.

3 Numerical details

The KRR function (1) is trained to reconstruct the mass residuals, i.e., the deviations $M_{\text{res}}(N, Z) = M_{\text{exp}}(N, Z) - M_{\text{th}}(N, Z)$ between the experimental data M_{exp} and theoretical predictions M_{th} for a given mass model. Once the weights w_i are obtained, the reconstructed function $S(N, Z)$ can be calculated with Eq. 1 for every nucleus (N, Z) . The predicted mass for a nucleus (N, Z) is, thus, given by $M_{\text{KRR}} = M_{\text{th}}(N, Z) + S(N, Z)$.

The experimental masses M_{exp} are taken from the AME2020 [4], while only those nuclei with $Z, N \geq 8$ and experimental errors $\sigma^{\text{exp}} < 100$ keV are considered. There are totally 2340 data composing the entire data set. The theoretical masses M_{th} are taken from the mass table WS4 [7].

One of the hyperparameters, i.e., penalty strength λ , had been carefully validated to be 0.3 for the KRR study of nuclear masses in Ref. [36], which would be adopted in this study.

4 Results and discussion

The main purpose of this work is to compare the performances of different kernel functions in the KRR approach for nuclear mass predictions. The performances are illustrated by comparing the accuracies of describing experimentally known nuclei and the extrapolation abilities, through the leave-one-out cross-validation and the extrapolation validation.

4.1 Leave-one-out cross-validation

The leave-one-out cross-validation is adopted to evaluate the accuracy of the KRR approach with different given types of kernel functions. In the leave-one-out cross-validation, for a given set of hyperparameters (σ, λ) , the mass prediction for each of the 2,340 nuclei

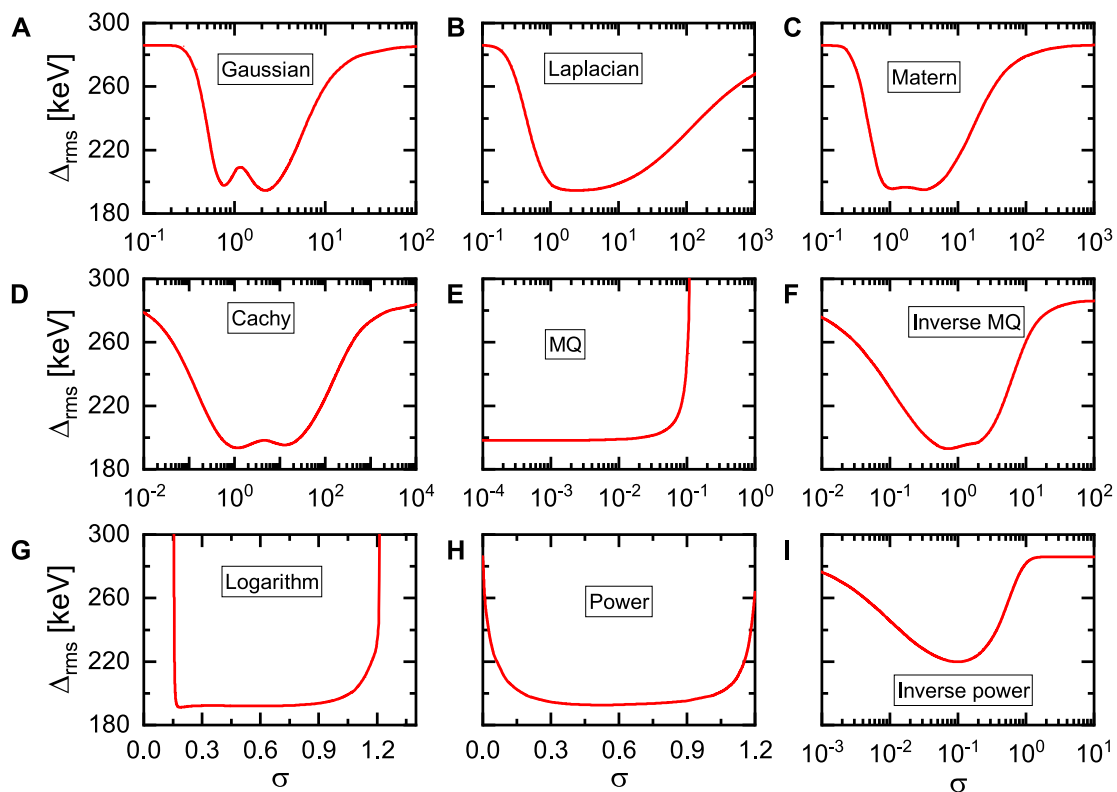


FIGURE 1

The Δ_{rms} between the KRR predictions with different kernels (A-I for nine different kernels) and the experimental data as functions of the corresponding hyperparameter σ .

TABLE 1 The minima of the Δ_{rms} (in unit of keV) and the corresponding hyperparameters in the leave-one-out cross-validation for the KRR approach with different kernels.

Kernels	Gaussian	Laplacian	Matern	Cachy	MQ	Inverse MQ	Logarithm	Power	Inverse power
σ	2.2	2.4	3.2	1.2	0	0.7	0.2	0.6	0.1
Δ_{rms} (all)	195	195	195	194	198	193	191	193	220
Δ_{rms} (ee)	203	202	203	198	203	198	197	199	225
Δ_{rms} (eo)	180	180	180	180	188	179	177	178	211
Δ_{rms} (oe)	173	172	172	173	179	172	170	171	203
Δ_{rms} (oo)	219	221	221	220	220	219	217	220	240

is obtained by the KRR network trained on all other 2,339 nuclei. The rms deviation Δ_{rms} between experimental and predicted masses of the 2,340 nuclei is calculated and regarded as a measure of the accuracy.

There are mainly two advantages of the leave-one-out cross-validation. First, it avoids the randomness caused by the random sampling in the validation-set method. Second, it matches the idea that when one wants to predict the mass of an unknown nucleus, information of all the other nuclei with experimentally known masses would be considered to build the model.

In Figure 1, the Δ_{rms} between the KRR predictions with different kernels and the experimental data are shown as functions of the

corresponding hyperparameter σ , respectively. The minima of the Δ_{rms} between the experimental data and the theoretical nuclear mass predictions, as shown in Figure 1 for every kernels, are listed in Table 1, together with the corresponding hyperparameters σ .

As can be seen in both Figure 1; Table 1, if the hyperparameters σ are adjusted to proper values respectively, the KRR approach with most of the kernels can reduce the Δ_{rms} to similar level around 195 keV, except for the one with inverse power kernel, which reduces the Δ_{rms} to 220 keV. Note that for the MQ kernel $K(r) = \sqrt{r^2 + \sigma^2}$, the predictions with smaller σ gives smaller Δ_{rms} , which indeed reduces to be the linear kernel $K(r) = r$ when $\sigma = 0$. It is also noted that the Δ_{rms} increases rapidly

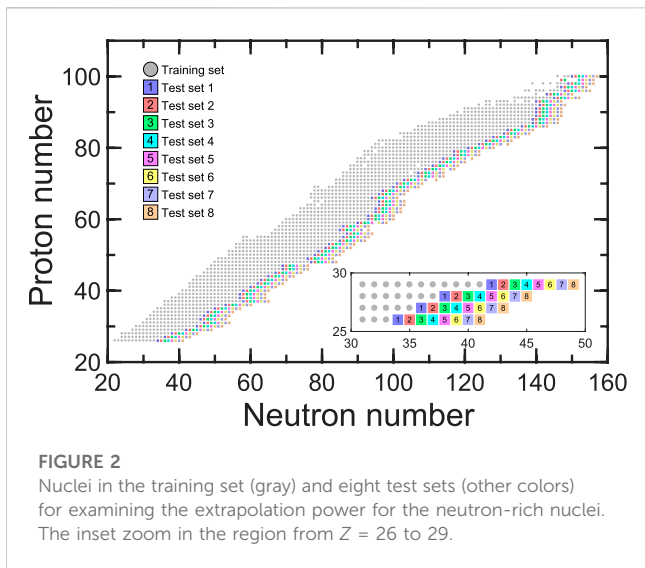


FIGURE 2
Nuclei in the training set (gray) and eight test sets (other colors) for examining the extrapolation power for the neutron-rich nuclei. The inset zoom in the region from $Z = 26$ to 29 .

as the decrease of the hyperparameter σ of the logarithm kernel approaching small values. This is because that the Logarithm kernel $K(r) = \ln(r^2 + 1)$ would approach to a constant $\ln(2)$ and lose the predicted power, when the σ is taken as a small value.

It is found that the predictions of the even-odd (eo) and odd-even (oe) nuclei are more accurate than the predictions of the even-even (ee) and odd-odd (oo) nuclei, which holds true for all the kernels. This is

because the KRR prediction generates a smooth nuclear mass surface, which tends to average the predictions of all the nuclear masses. Generally speaking, the ee nuclei are most bound and the oo nuclei are least bound, while the eo and oe nuclei are in-between. Therefore, the smooth KRR prediction tends to have better descriptions of the eo and oe nuclei. If one wants to well capture the odd-even effects and improve the nuclear mass predictions in the framework of KRR approach, the adopted kernel function should be remodulated to include the odd-even effects [37]. As is known, the shell effects commonly have an energy change of about 10 MeV between a magic nucleus and its mid-shell isotopes. Therefore, it is naturally believed that the shell effects can be captured by the KRR approach with precision of 195 keV.

The results from the leave-one-out cross-validation indicate that the KRR approach with different kernels can reach similar accuracies in interpolation or very short extrapolation, if proper values of hyperparameters are adopted. Therefore, in the applications of predicting nuclear masses for the nuclei that very close to the experimentally known region, the choices of different kernel functions may hardly affect the prediction accuracy.

4.2 Extrapolation validation

In order to examine the extrapolation abilities of the KRR approaches with different kernels, the set of nuclei with known masses is redivided as shown in Figure 2. For each isotopic chain of $Z \geq 26$, the eight most neutron-rich nuclei are removed out from the

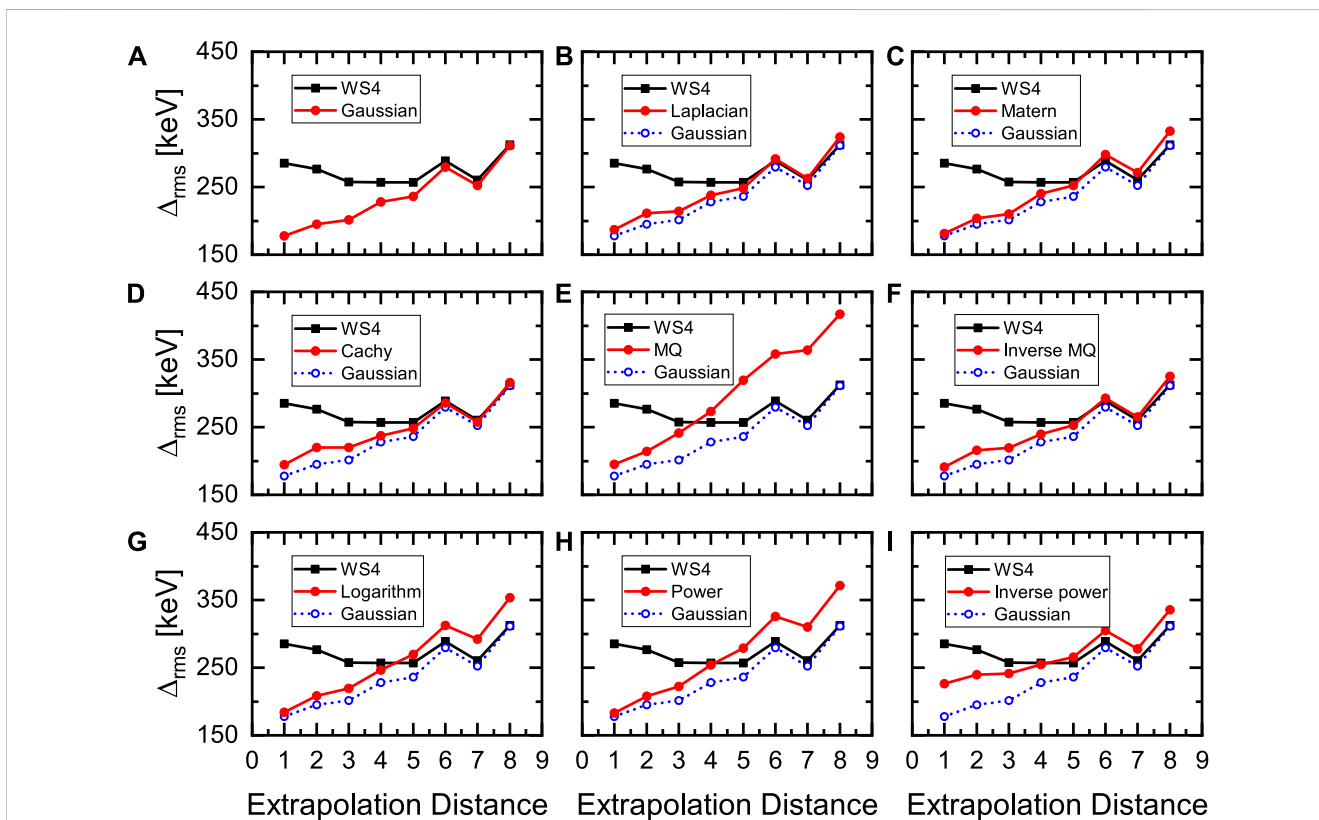


FIGURE 3
Comparison of the extrapolation power of the KRR approach with different kernels (A-I for nine different kernels) for eight test sets with different extrapolation distances.

training set, and they are classified into eight test sets respectively, corresponding to the different extrapolation distances from the remain training set in the neutron direction. This is the similar as the division in Refs. [36], but for $Z \geq 26$. The rms deviations Δ_{rms} between the experimental and predicted masses of the eight test sets would be taken as a measure to compare the extrapolation abilities.

Figure 3 shows the Δ_{rms} of the eight test sets for the KRR approach with different kernels adopting the corresponding hyperparameters listed in Table 1, in comparison with the ones for the WS4 mass model. First of all, for the case of short extrapolation, i.e., extrapolation distance smaller than four, the KRR approach with all of the adopted kernels can reduce the Δ_{rms} obtained by the WS4 mass model. For the test sets with large extrapolation distances, i.e., extrapolation distance larger than four, the KRR approach with the MQ, logarithm, and power kernels obviously worsen the WS4 predictions. This is due to the fact that the corrections for the MQ, logarithm, and power kernels increase with the increasing of the Euclidean norm r . While, for the other six kernels, the corrections decrease with the increasing of the Euclidean norm r , which give them the abilities to reduce the risk of worsening the mass descriptions for nuclei at large extrapolation distances. The detail discussions can be seen in Ref. [36], where the Gaussian kernel is taken as an example.

The extrapolation performances of the KRR approach with the six kernels that the corrections decrease with the increasing of the Euclidean norm r are similar, except for the inverse power kernel. They can improve the mass predictions of the nuclei with extrapolation distance smaller than five, and reduce the risk of worsening mass predictions at large extrapolation distances. Among these adopted kernels, the performance of the Gaussian kernel is slightly better than other ones in the extrapolation validation for the whole range of the extrapolation distances. Therefore, the Gaussian kernel, which is commonly used in machine-learning, can be also taken as a default choice in the nuclear mass predictions.

5 Summary

The performances of different kernel functions, i.e., Gaussian, Laplacian, Matern, Cachy, Multiquadric, inverse Multiquadric, Logarithm, power, and inverse power kernels, in nuclear mass predictions with the KRR approach in describing experimentally known nuclei and extrapolating to neutron-rich nuclei are compared. The comparison is performed through the leave-one-out cross-validation and the extrapolation validation. From the leave-one-out cross-validation, it is found that the KRR approach with most of the kernels can reduce the Δ_{rms} to similar level around 195 keV. From the extrapolation validation, it is found that the performances of the kernel functions strongly depend on its increasing/decreasing behaviors with respect to the Euclidean norm r . For the case that the kernel functions decrease with the increasing of the Euclidean norm r , the corresponding KRR predictions can reduce the risk of worsening the mass predictions for nuclei at large extrapolation distances. Among these adopted kernels, the performance of the Gaussian kernel is slightly better than other ones in the extrapolation validation for the whole range of the extrapolation distances. Therefore, it is suggested to be taken as the default choice in the nuclear mass predictions.

In the present study, only the masses are considered as the outputs to train the ML models, and thus the obtained ML models

are unable to predict other nuclear properties. However, the predictions of different nuclear properties by ML models at the same time can be achieved by the idea of multi-task learning. Multi-task learning (MTL) is a subfield of machine learning, in which multiple related learning tasks are solved at the same time by exploiting commonalities and differences across tasks. It has been successfully applied in nuclear physics, e.g., in the description of giant dipole resonance key parameters [58] and in the description of nuclear masses and separation energies [41]. It would be interesting to apply different kernels in the MTL framework in future works, in that case the performances and reliabilities of different kernels can be evaluated on additional nuclear properties.

Data availability statement

Publicly available datasets were analyzed in this study. This data can be found here: https://www-nds.iaea.org/amdc/ame2020/mass_1.mas20.txt; <http://www.imqmd.com/mass/WS4.txt>.

Author contributions

XW conceived the idea, performed the calculations, and wrote the manuscript.

Funding

This work was partly supported by the National Key R&D Program of China (Contracts No. 2018YFA0404400 and No. 2017YFE0116700), the National Natural Science Foundation of China (Grants No. 11875075, No. 11935003, No. 11975031, No. 12141501, and No. 12070131001), the China Postdoctoral Science Foundation under Grant No. 2021M700256, and the High-performance Computing Platform of Peking University.

Acknowledgments

XW acknowledges P. W. Zhao and L. H. Guo for helpful discussions.

Conflict of interest

The author declares that the research was conducted in the absence of any commercial or financial relationships that could be construed as a potential conflict of interest.

Publisher's note

All claims expressed in this article are solely those of the authors and do not necessarily represent those of their affiliated organizations, or those of the publisher, the editors and the reviewers. Any product that may be evaluated in this article, or claim that may be made by its manufacturer, is not guaranteed or endorsed by the publisher.

References

- Lunney D, Pearson JM, Thibault C. Recent trends in the determination of nuclear masses. *Rev Mod Phys* (2003) 75:1021–82. doi:10.1103/RevModPhys.75.1021
- Burbidge EM, Burbidge GR, Fowler WA, Hoyle F. Synthesis of the elements in stars. *Rev Mod Phys* (1957) 29:547–650. doi:10.1103/RevModPhys.29.547
- Mumpower M, Surman R, McLaughlin G, Aprahamian A. The impact of individual nuclear properties on r-process nucleosynthesis. *Prog Part Nucl Phys* (2016) 86:86–126. doi:10.1016/j.pnpnp.2015.09.001
- Wang M, Huang W, Kondev F, Audi G, Naimi S. The AME 2020 atomic mass evaluation (II). tables, graphs and references. *Chin Phys C* (2021) 45:030003. doi:10.1088/1674-1137/abddaf
- Weizsäcker C. Zur theorie der kernmassen. *Z Physik* (1935) 96:431–58. doi:10.1007/BF01337700
- Möller P, Sierk A, Ichikawa T, Sagawa H. Nuclear ground-state masses and deformations: Frdm(2012). *Atom Data Nucl Data Tables* (2016) 109:1–204. doi:10.1016/j.adt.2015.10.002
- Wang N, Liu M, Wu X, Meng J. Surface diffuseness correction in global mass formula. *Phys Lett B* (2014) 734:215–9. doi:10.1016/j.physletb.2014.05.049
- Goriely S, Chamel N, Pearson JM. Further explorations of skyrme-Hartree-Fock-bogoliubov mass formulas. xiii. the 2012 atomic mass evaluation and the symmetry coefficient. *Phys Rev C* (2013) 88:024308. doi:10.1103/PhysRevC.88.024308
- Geng LS, Toki H, Meng J. Masses, deformations and charge radii—nuclear ground-state properties in the relativistic mean field model. *Prog Theor Phys* (2005) 113:785–800. doi:10.1143/PTP.113.785
- Xia X, Lim Y, Zhao P, Liang H, Qu X, Chen Y, et al. The limits of the nuclear landscape explored by the relativistic continuum hartree-bogoliubov theory. *Atom Data Nucl Data Tables* (2018) 121–122:1–215. doi:10.1016/j.adt.2017.09.001
- Goriely S, Chamel N, Pearson JM. Skyrme-Hartree-Fock-bogoliubov nuclear mass formulas: Crossing the 0.6 mev accuracy threshold with microscopically deduced pairing. *Phys Rev Lett* (2009) 102:152503. doi:10.1103/PhysRevLett.102.152503
- Erler J, Birge N, Kortelainen M, Nazarewicz W, Olsen E, Perhac AM, et al. The limits of the nuclear landscape. *Nature* (2012) 486:509–12. doi:10.1038/nature11188
- Afnasjev A, Agbemava S, Ray D, Ring P. Nuclear landscape in covariant density functional theory. *Phys Lett B* (2013) 726:680–4. doi:10.1016/j.physletb.2013.09.017
- Lu KQ, Li ZX, Li ZP, Yao JM, Meng J. Global study of beyond-mean-field correlation energies in covariant energy density functional theory using a collective Hamiltonian method. *Phys Rev C* (2015) 91:027304. doi:10.1103/PhysRevC.91.027304
- Yang YL, Wang YK, Zhao PW, Li ZP. Nuclear landscape in a mapped collective Hamiltonian from covariant density functional theory. *Phys Rev C* (2021) 104:054312. doi:10.1103/PhysRevC.104.054312
- Zhang K, Cheoun M-K, Choi Y-B, Chong PS, Dong J, Dong Z, et al. Nuclear mass table in deformed relativistic hartree-bogoliubov theory in continuum. i: Even-even nuclei. *Atom Data Nucl Data Tables* (2022) 144:101488. doi:10.1016/j.adt.2022.101488
- Pan C, Cheoun M-K, Choi Y-B, Dong J, Du X, Fan X-H, et al. Deformed relativistic hartree-bogoliubov theory in continuum with a point-coupling functional. ii. examples of odd nd isotopes. *Phys Rev C* (2022) 106:014316. doi:10.1103/PhysRevC.106.014316
- Kirson MW. Mutual influence of terms in a semi-empirical mass formula. *Nucl Phys A* (2008) 798:29–60. doi:10.1016/j.nuclphysa.2007.10.011
- Mumpower MR, Surman R, Fang D-L, Beard M, Möller P, Kawano T, et al. Impact of individual nuclear masses on r-process abundances. *Phys Rev C* (2015) 92:035807. doi:10.1103/PhysRevC.92.035807
- Jiang XF, Wu XH, Zhao PW. Sensitivity study of r-process abundances to nuclear masses. *Astrophys J* (2021) 915:29. doi:10.3847/1538-4357/ac042f
- Duflo J, Zuker A. Microscopic mass formulas. *Phys Rev C* (1995) 52:R23–7. doi:10.1103/PhysRevC.52.R23
- Pearson J, Nayak R, Goriely S. Nuclear mass formula with bogolyubov-enhanced shell-quenching: Application to r-process. *Phys Lett B* (1996) 387:455–9. doi:10.1016/0370-2693(96)01071-4
- Koura H, Tachibana T, Uno M, Yamada M. Nuclidic mass formula on a spherical basis with an improved even-odd term. *Prog Theor Phys* (2005) 113:305–25. doi:10.1143/PTP.113.305
- Carleo G, Cirac I, Cranmer K, Daudet L, Schuld M, Tishby N, et al. Machine learning and the physical sciences. *Rev Mod Phys* (2019) 91:045002. doi:10.1103/RevModPhys.91.045002
- Boehnlein A, Diefenthaler M, Sato N, Schram M, Ziegler V, Fanelli C, et al. Colloquium: Machine learning in nuclear physics. *Rev Mod Phys* (2022) 94:031003. doi:10.1103/RevModPhys.94.031003
- Gazula S, Clark J, Bohr H. Learning and prediction of nuclear stability by neural networks. *Nucl Phys A* (1992) 540:1–26. doi:10.1016/0375-9474(92)90191-L
- Gernoth K, Clark J, Prater J, Bohr H. Neural network models of nuclear systematics. *Phys Lett B* (1993) 300:1–7. doi:10.1016/0370-2693(93)90738-4
- Wang N, Liu M. Nuclear mass predictions with a radial basis function approach. *Phys Rev C* (2011) 84:051303. doi:10.1103/PhysRevC.84.051303
- Niu ZM, Zhu ZL, Niu YF, Sun BH, Heng TH, Guo JY. Radial basis function approach in nuclear mass predictions. *Phys Rev C* (2013) 88:024325. doi:10.1103/PhysRevC.88.024325
- Zhang HF, Wang LH, Yin JP, Chen PH, Zhang HF. Performance of the levenberg-marquardt neural network approach in nuclear mass prediction. *J Phys G-nucl Part Phys* (2017) 44:045110. doi:10.1088/1361-6471/aa5d78
- Utama R, Piekarewicz J, Prosper HB. Nuclear mass predictions for the crustal composition of neutron stars: A bayesian neural network approach. *Phys Rev C* (2016) 93:014311. doi:10.1103/PhysRevC.93.014311
- Niu ZM, Liang HZ. Nuclear mass predictions based on bayesian neural network approach with pairing and shell effects. *Phys Lett B* (2018) 778:48–53. doi:10.1016/j.physletb.2018.01.002
- Neufcourt L, Cao YC, Nazarewicz W, Viens F. Bayesian approach to model-based extrapolation of nuclear observables. *Phys Rev C* (2018) 98:034318. doi:10.1103/PhysRevC.98.034318
- Pastore A, Neill D, Powell H, Medler K, Barton C. Impact of statistical uncertainties on the composition of the outer crust of a neutron star. *Phys Rev C* (2020) 101:035804. doi:10.1103/PhysRevC.101.035804
- Idini A. Statistical learnability of nuclear masses. *Phys Rev Res* (2020) 2:043363. doi:10.1103/PhysRevResearch.2.043363
- Wu D, Bai CL, Sagawa H, Zhang HQ. Calculation of nuclear charge radii with a trained feed-forward neural network. *Phys Rev C* (2020) 102:054323. doi:10.1103/PhysRevC.102.054323
- Wu XH, Guo LH, Zhao PW. Nuclear masses in extended kernel ridge regression with odd-even effects. *Phys Lett B* (2021) 819:136387. doi:10.1016/j.physletb.2021.136387
- Shelley M, Pastore A. A new mass model for nuclear astrophysics: Crossing 200 keV accuracy. *Universe* (2021) 7:131. doi:10.3390/universe7050131
- Gao ZP, Wang YJ, Lü HL, Li QF, Shen CW, Liu L. Machine learning the nuclear mass. *Nucl Sci Tech* (2021) 32:109. doi:10.1007/s41365-021-00956-1
- Liu Y, Su C, Liu J, Danielewicz P, Xu C, Ren Z. Improved naive bayesian probability classifier in predictions of nuclear mass. *Phys Rev C* (2021) 104:014315. doi:10.1103/PhysRevC.104.014315
- Wu X, Lu Y, Zhao P. Multi-task learning on nuclear masses and separation energies with the kernel ridge regression. *Phys Lett B* (2022) 834:137394. doi:10.1016/j.physletb.2022.137394
- Akkoyun S, Bayram T, Kara SO, Sinan A. An artificial neural network application on nuclear charge radii. *J Phys G-nucl Part Phys* (2013) 40:055106. doi:10.1088/0954-3899/40/5/055106
- Utama R, Chen W-C, Piekarewicz J. Nuclear charge radii: Density functional theory meets bayesian neural networks. *J Phys G-nucl Part Phys* (2016) 43:114002. doi:10.1088/0954-3899/43/11/114002
- Ma Y, Su C, Liu J, Ren Z, Xu C, Gao Y. Predictions of nuclear charge radii and physical interpretations based on the naive bayesian probability classifier. *Phys Rev C* (2020) 101:014304. doi:10.1103/PhysRevC.101.014304
- Ma J-Q, Zhang Z-H. Improved phenomenological nuclear charge radius formulae with kernel ridge regression. *Chin Phys C* (2022) 46:074105. doi:10.1088/1674-1137/ac6154
- Niu ZM, Fang JY, Niu YF. Comparative study of radial basis function and bayesian neural network approaches in nuclear mass predictions. *Phys Rev C* (2019) 100:054311. doi:10.1103/PhysRevC.100.054311
- Lovell AE, Nunes FM, Catacora-Rios M, King GB. Recent advances in the quantification of uncertainties in reaction theory. *J Phys G-nucl Part Phys* (2020) 48:014001. doi:10.1088/1361-6471/abba72
- Ma C-W, Peng D, Wei H-L, Niu Z-M, Wang Y-T, Wada R. Isotopic cross-sections in proton induced spallation reactions based on the bayesian neural network method. *Chin Phys C* (2020) 44:014104. doi:10.1088/1674-1137/44/1/014104
- Wu D, Bai CL, Sagawa H, Nishimura S, Zhang HQ. β -delayed one-neutron emission probabilities within a neural network model. *Phys Rev C* (2021) 104:054303. doi:10.1103/PhysRevC.104.054303
- Saxena G, Sharma PK, Saxena P. Modified empirical formulas and machine learning for α -decay systematics. *J Phys G-nucl Part Phys* (2021) 48:055103. doi:10.1088/1361-6471/abcd1c
- Neudecker D, Cabellos O, Clark AR, Grosskopf MJ, Haeck W, Herman MW, et al. Informing nuclear physics via machine learning methods with differential and integral experiments. *Phys Rev C* (2021) 104:034611. doi:10.1103/PhysRevC.104.034611
- Wang X, Zhu L, Su J. Modeling complex networks of nuclear reaction data for probing their discovery processes. *Chin Phys C* (2021) 45:124103. doi:10.1088/1674-1137/ac23d5
- Huang TX, Wu XH, Zhao PW. Application of kernel ridge regression in predicting neutron-capture reaction cross-sections. *Commun Theor Phys* (2022) 74:095302. doi:10.1088/1572-9494/ac763b

54. Jiang WG, Hagen G, Papenbrock T. Extrapolation of nuclear structure observables with artificial neural networks. *Phys Rev C* (2019) 100:054326. doi:10.1103/PhysRevC.100.054326
55. Lasserri R-D, Regnier D, Ebran J-P, Penon A. Taming nuclear complexity with a committee of multilayer neural networks. *Phys Rev Lett* (2020) 124:162502. doi:10.1103/PhysRevLett.124.162502
56. Yoshida S. Nonparametric bayesian approach to extrapolation problems in configuration interaction methods. *Phys Rev C* (2020) 102:024305. doi:10.1103/PhysRevC.102.024305
57. Wang X, Zhu L, Su J. Providing physics guidance in bayesian neural networks from the input layer: The case of giant dipole resonance predictions. *Phys Rev C* (2021) 104:034317. doi:10.1103/PhysRevC.104.034317
58. Bai J, Niu Z, Sun B, Niu Y. The description of giant dipole resonance key parameters with multitask neural networks. *Phys Lett B* (2021) 815:136147. doi:10.1016/j.physletb.2021.136147
59. Neufcourt L, Cao Y, Nazarewicz W, Olsen E, Viens F. Neutron drip line in the ca region from bayesian model averaging. *Phys Rev Lett* (2019) 122:062502. doi:10.1103/PhysRevLett.122.062502
60. Neufcourt L, Cao Y, Giuliani SA, Nazarewicz W, Olsen E, Tarasov OB. Quantified limits of the nuclear landscape. *Phys Rev C* (2020) 101:044307. doi:10.1103/PhysRevC.101.044307
61. Wang Z-A, Pei J, Liu Y, Qiang Y. Bayesian evaluation of incomplete fission yields. *Phys Rev Lett* (2019) 123:122501. doi:10.1103/PhysRevLett.123.122501
62. Lovell AE, Mohan AT, Talou P. Quantifying uncertainties on fission fragment mass yields with mixture density networks. *J Phys G-nucl Part Phys* (2020) 47:114001. doi:10.1088/1361-6471/ab9f58
63. Qiao CY, Pei JC, Wang ZA, Qiang Y, Chen YJ, Shu NC, et al. Bayesian evaluation of charge yields of fission fragments of ^{239}U . *Phys Rev C* (2021) 103:034621. doi:10.1103/PhysRevC.103.034621
64. Wang R, Ma Y-G, Wada R, Chen L-W, He W-B, Liu H-L, et al. Nuclear liquid-gas phase transition with machine learning. *Phys Rev Res* (2020) 2:043202. doi:10.1103/PhysRevResearch.2.043202
65. Keeble J, Rios A. Machine learning the deuteron. *Phys Lett B* (2020) 809:135743. doi:10.1016/j.physletb.2020.135743
66. Adams C, Carleo G, Lovato A, Rocco N. Variational Monte Carlo calculations of $a \leq 4$ nuclei with an artificial neural-network correlator ansatz. *Phys Rev Lett* (2021) 127:022502. doi:10.1103/PhysRevLett.127.022502
67. Wu XH, Ren ZX, Zhao PW. Nuclear energy density functionals from machine learning. *Phys Rev C* (2022) 105:L031303. doi:10.1103/PhysRevC.105.L031303
68. Niu ZM, Sun BH, Liang HZ, Niu YF, Guo JY. Improved radial basis function approach with odd-even corrections. *Phys Rev C* (2016) 94:054315. doi:10.1103/PhysRevC.94.054315
69. Ma NN, Zhang HF, Yin P, Bao XJ, Zhang HF. Weizsäcker-skyrme-type nuclear mass formula incorporating two combinatorial radial basis function prescriptions and their application. *Phys Rev C* (2017) 96:024302. doi:10.1103/PhysRevC.96.024302
70. Niu ZM, Liang HZ, Sun BH, Niu YF, Guo JY, Meng J. High precision nuclear mass predictions towards a hundred kilo-electron-volt accuracy. *Sci Bull* (2018) 63:759–64. doi:10.1016/j.scib.2018.05.009
71. Li T, Wei H, Liu M, Wang N. Ability of the radial basis function approach to extrapolate nuclear mass. *Commun Theor Phys* (2021) 73:095301. doi:10.1088/1572-9494/ac08fa
72. Niu ZM, Liang HZ. Nuclear mass predictions with machine learning reaching the accuracy required by r -process studies. *Phys Rev C* (2022) 106:L021303. doi:10.1103/PhysRevC.106.L021303
73. Guo L, Wu X, Zhao P. Nuclear mass predictions of the relativistic density functional theory with the kernel ridge regression and the application to r -process simulations. *Symmetry* (2022) 14:1078. doi:10.3390/sym14061078